

Emplacement of nested diapirs: Results of centrifuge modelling

C. DIETL¹ AND H. A. KOYI²

¹ *Geology and Geochemistry Department, Stockholm University, S-10691 Stockholm, Sweden*

² *Hans Ramberg Tectonic Lab, Dept. of Earth Sciences, Uppsala University, Villavägen 16, 75236 Uppsala, Sweden*

Abstract: Concentrically expanded plutons (CEPs) are characterized by compositional zoning, mainly concentric magmatic fabric within the pluton and ductile fabric in the contact aureole concordant with the pluton/host rock contact. Two intrusion mechanisms have been proposed for CEPs: dyking + ballooning and diapirism. Here, we present results of a centrifuge model to study the kinematics and dynamics of CEPs. The model was centrifuged twice. For each stage one buoyant layer - each with the same physical parameters - was attached to the bottom of the model. After the first stage, diapirs of a blue stained buoyant layer intruded and deformed the overburden to spread as mushroom-shaped diapirs below a less-dense upper layer. After second centrifuging with a red buoyant layer attached, an intrusion of this buoyant material occurred along the stem of the pre-existing diapirs using them as a mechanically weak pathway. This latter intrusion was not diapiric, but the buoyant material rose as a “ductile dyke”. Once reaching the bulb of the pre-existing diapirs, the intrusive material spread laterally resulting in extensive spreading and expansion of the overhang of the pre-existing diapirs. Model results show that CEPs can be the result of combined initial diapirism and subsequent “ductile dyking”. Multiple diapirs can form only when the overburden units deform ductilely during the different stages of diapirism.

Introduction

Concentrically expanded plutons (CEPs) are a common igneous feature. Paterson and Vernon (1995) defined CEPs as plutons with a distinct zoning either with a mafic rim phase getting more felsic towards their centers (normal zoning) or vice versa with a felsic rim and a mafic core (reverse zoning). Commonly flattened enclaves are found near the margins of the plutons. Structures in the immediate country rocks are deflected into parallelism with the pluton margins and ductile deformation is a common feature in the contact aureole. In both the pluton and the host rock intensity of the foliation increases toward the pluton/host rock contact.

Generally, two intrusion mechanisms are proposed for CEPs. The first proposed process combines dyking as an ascent mechanism with ballooning as the emplacement process *sensu strictu* (e.g. Petford 1996). According to this idea CEPs are constructed by numerous dykes which feed the same magma chamber often using the same conduit as pathway for the magma. Dyking is defined as the upward movement of a fluid phase through the elastic fracturing of rocks driven by the high magma pressure and buoyancy (Lister and Kerr 1991). Dykes usually propagate perpendicular to the least principal stress and follow zones of weakness in the rocks they travel through. They form a conduit with a large lateral extent relative to its thickness (Spera 1980). The emplacement of multiple dyke-fed magma batches to the same magma chamber leads to magma chamber expansion or “ballooning” (e.g. Molyneux and Hutton 2000): host rocks of the pluton

deform ductilely and the magma chamber inflates radially and relatively symmetrical as a result of the intrusion pressure of the intruding magma (Ramsay 1989, Paterson and Vernon 1995).

Diapirism is the upwelling of relative mobile material (e.g. magma) through overlying rocks (Van den Eekhout et al. 1986) and has also been proposed as a mechanism for the ascent and emplacement of CEPs (e.g. Miller and Paterson 1999). The driving force of diapirism is buoyancy. Diapiric plutons are generally regarded as the result of the buoyant rise of an elliptically shaped body of magma. Multiple bodies of magma intruding subsequently as diapirs into the same region / space are also referred to as nested diapirs (Paterson and Vernon 1995). They can be described as diapir-in-diapir structures, where earlier magma bodies are intruded by subsequent diapirs of possibly different composition.

Natural examples of CEPs include the Devonian Ardara pluton (Fig. 1) in Ireland that intruded into a depth of ca. 7-9 km (Kerrick 1987). The pluton is normally zoned from quartzmonzodiorite at the rim through tonalite to granodiorite in the core. The magmatic foliation crosscuts internal contacts. It is parallel with the pluton / host rock interface in some parts of the pluton and discordant in others. Country rock markers such as bedding planes and pre-intrusive faults are deflected into parallelism with the contact only close to the pluton. At the southwestern margin a ductile shear zone is developed which incorporates both the host rock and the pluton, which is elongated along the shear zone (Paterson and Vernon 1995).

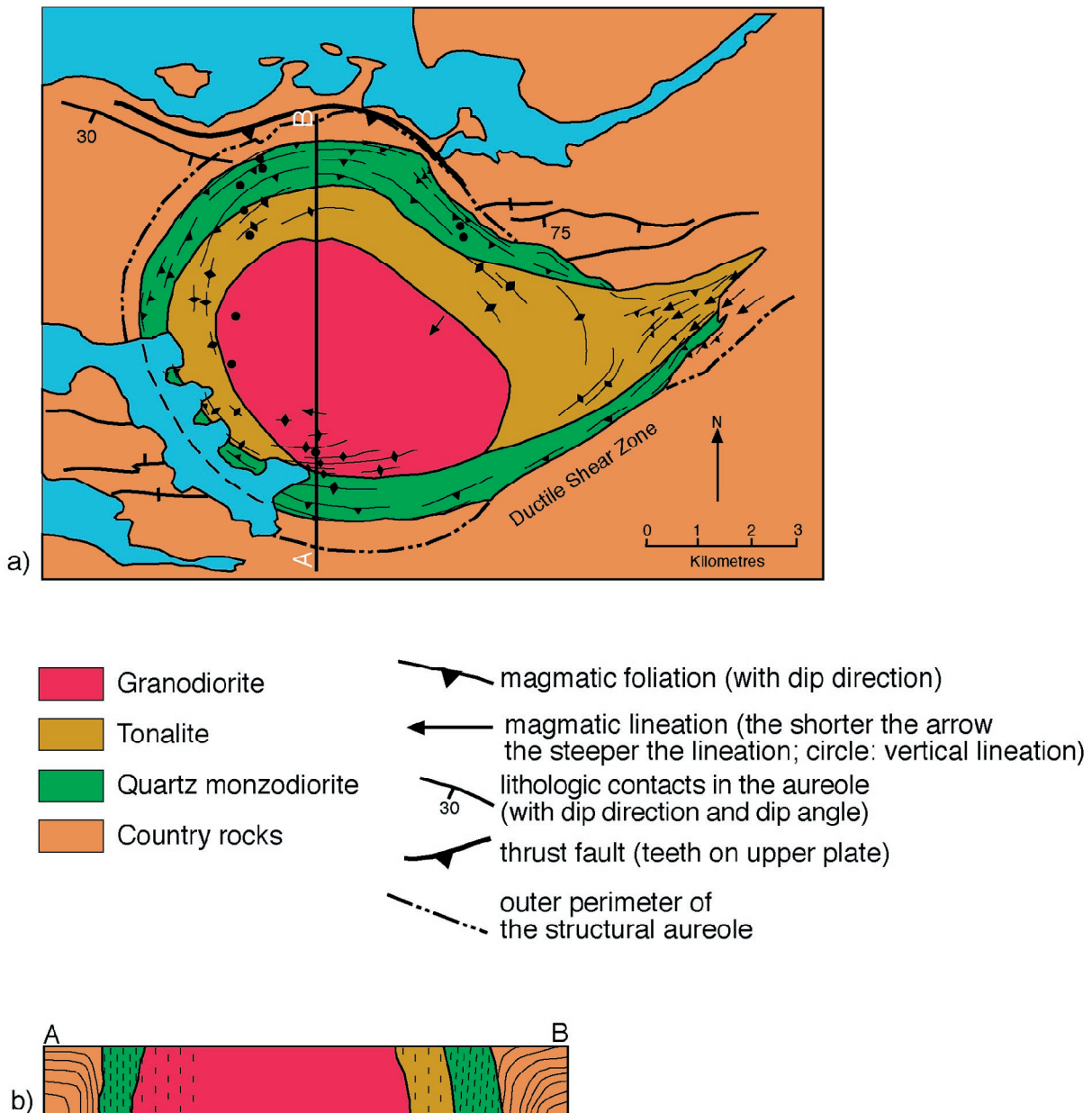


Figure 1. a) Simplified geologic map of the Ardara pluton (redrawn from Paterson and Vernon 1995). **b)** Cross section through the Ardara pluton along line A-B in Fig. 1a, based on data from Paterson and Vernon (1995) and Pitcher and Berger (1972). Colours from the legend in Fig. 1a, country rock markers as thin solid lines, magmatic foliation as thin dashed lines. Intensity of the magmatic foliation is indicated by the spacing between the lines.

The Permian (Bultitude and Champion 1992) Cannibal Creek pluton (Fig. 2) in Australia was emplaced into a depth of 7 to 9 km (Bateman 1985a). The pluton is not zoned, but consists of granite with K-Feldspar megacrysts. The granite is crosscut by megacrystic granodioritic to equigranular granitic ring dykes. Moreover, equigranular microgranitic dikes encircle the pluton almost completely (Bateman 1985b). A magmatic and perfectly contact parallel magmatic foliation is developed within the pluton. Country rock markers such as bedding and a bedding parallel foliation are deflected towards parallelism with the contact in almost the entire aureole. The pluton has discordant contacts with the host rocks only at its northern and southern ends (Paterson and Vernon 1995).

The Cretaceous Tuolumne intrusive suite (depth of

emplacement: 4-8 km, Bateman 1992) comprises a normal zoning with dark, fine grained and well foliated granodiorites at the rim and light, coarse grained and weakly foliated granodiorites and granite in the centre of the pluton (Bateman and Chappel 1979, Fig. 3). However, the steeply dipping magmatic foliation generally crosscuts intraplutonic contacts and strikes perpendicular to the longaxis of this stretched pluton. A contact parallel magmatic foliation was only observed within the southeastern protrusion of the pluton. The ductile host rock structures are bent into parallelism with the pluton/host rock contact at the southwestern and eastern margins of the intrusive suite. At the other contacts host rock structures are cut by the pluton (Paterson and Vernon 1995).

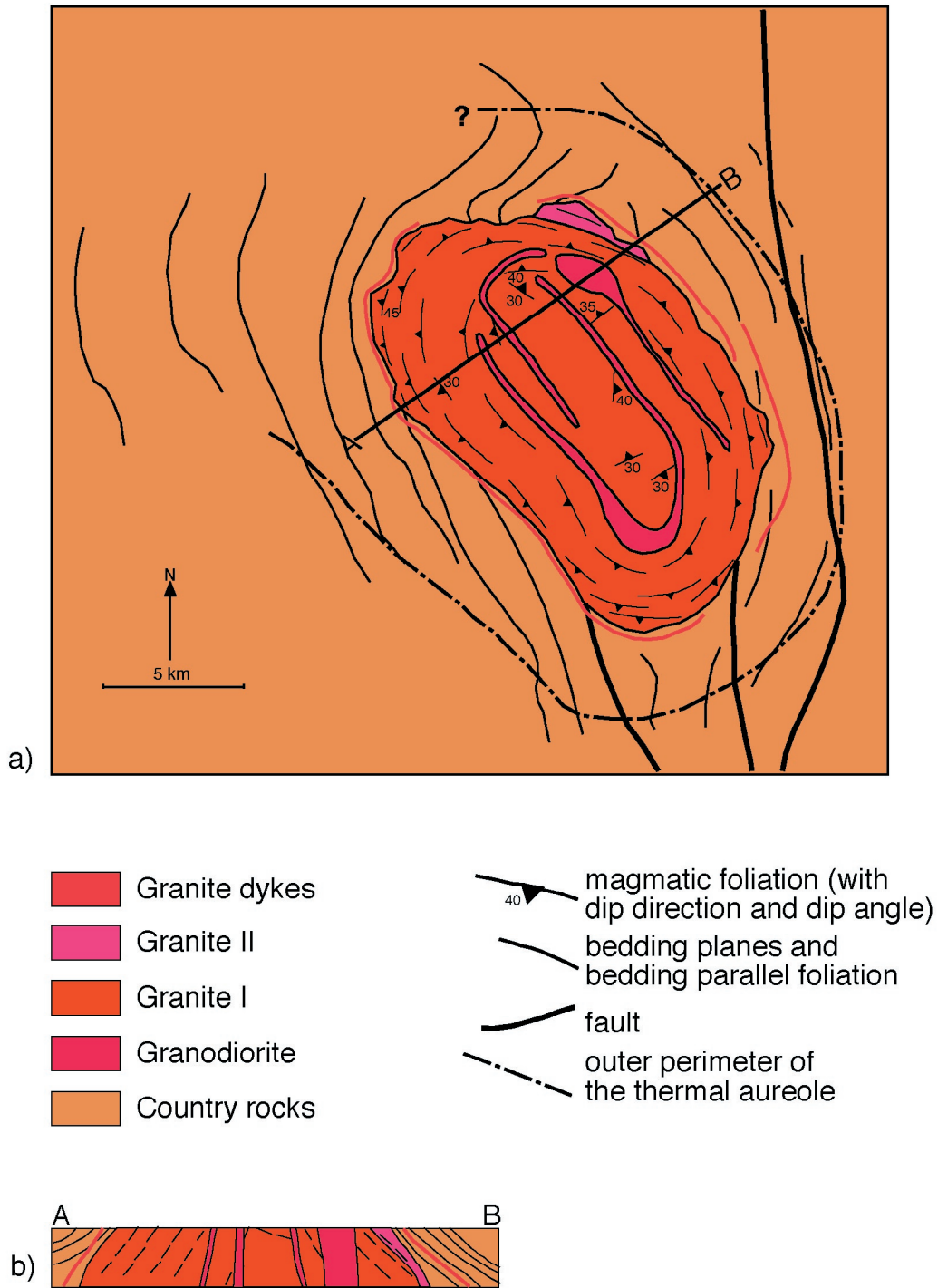


Figure 2. a) Simplified geologic map of the Cannibal Creek pluton (redrawn from Paterson and Vernon 1995). b) Cross section through the Cannibal Creek pluton along line A-B in Fig. 2a, based on data from Paterson and Vernon (1995), Paterson (1988) and Bateman (1985a). Colours from the legend in Fig. 2a, country rock markers as thin solid lines, magmatic foliation as thin dashed lines. Intensity of the magmatic foliation is indicated by the spacing between the lines.

Since all three plutons are excellent examples for CEPs both emplacement mechanism described above, including combinations of both, were proposed for their intrusion: Molyneux and Hutton (2000) proposed ballooning for the emplacement of the Ardara pluton, Bateman (1985a) suggested ballooning of a diapir for the Cannibal Creek pluton and Tikoff and Teyssier (1992) proposed dyke intrusion into a transpressional shear zone as emplacement mechanism for the Tuolumne intrusive suite. Paterson and

Vernon (1995) suggested diapirism by multiple processes for all three of them.

Here, we present results of a centrifuge model simulating multiple-stage melt intrusions to study the kinematics and dynamics of CEPs. We analyse the structures observed during the experiment and compare them with those observed in the above described major natural structures to draw conclusions about emplacement of CEPs.

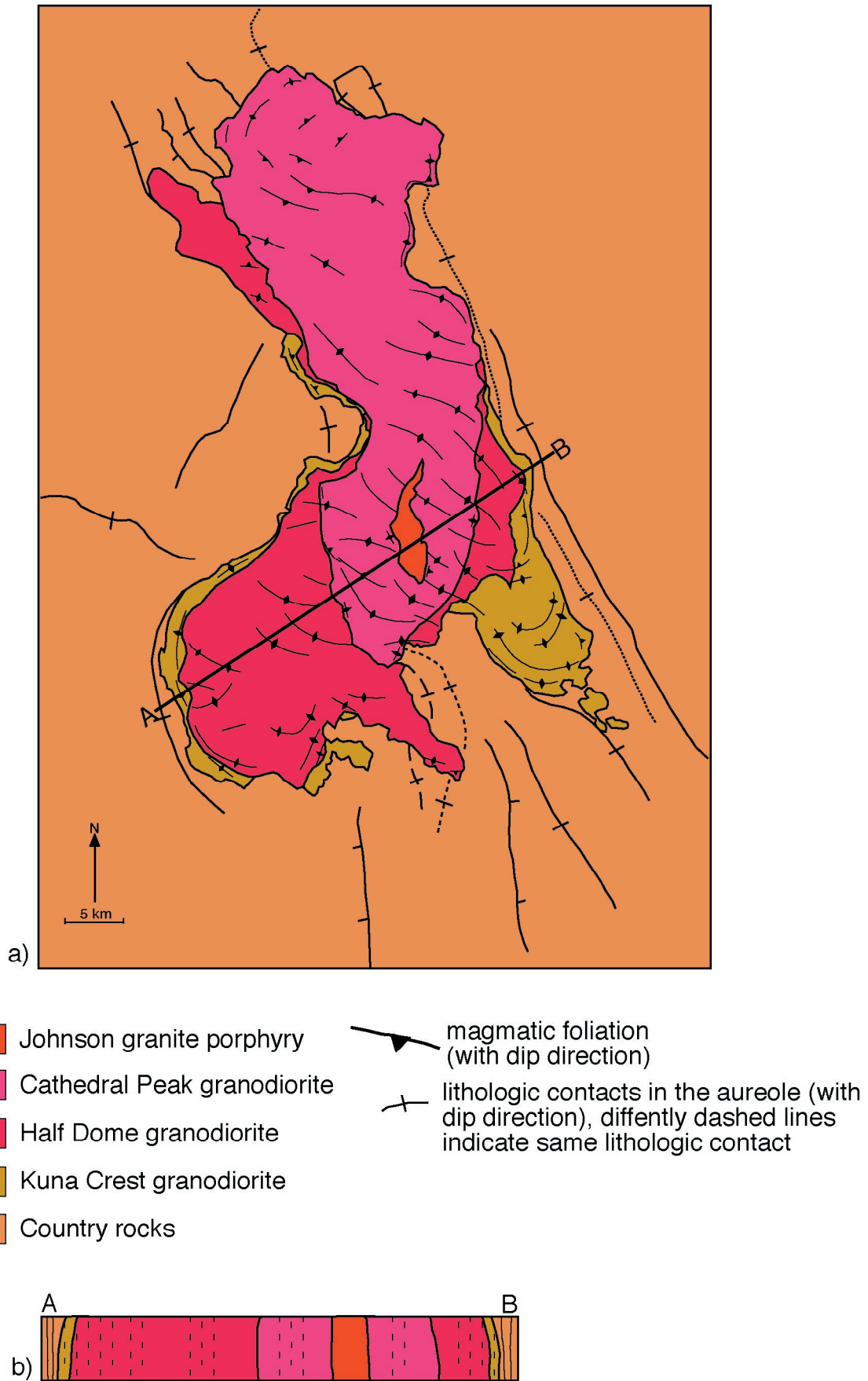


Figure 3. a) Simplified geologic map of the Tuolumne intrusive suite (redrawn from Paterson and Vernon 1995). b) Cross section through the Tuolumne intrusive suite along line A-B in Fig. 3a, based on data from Paterson and Vernon (1995). Colours from the legend in Fig. 3a, country rock markers as thin solid lines, magmatic foliation as thin dashed lines. Intensity of the magmatic foliation is indicated by the spacing between the lines.

The Experiment

The experiment was aimed to study the subsequent and independent rise of two buoyant layers and the resulting structures. For this purpose a two-stage model was developed. In the first stage a buoyant layer (stained blue) was overlain by an overburden, which consisted of passively coloured denser layers (Fig. 4). Overburden was passively stratified in order to visualise internal deformation. After the first centrifuging stage a second buoyant layer (stained red, but with the same physical properties as the first buoyant layer) was attached to the bottom boundary of the overburden and the model was centrifuged for a second time. After each centrifuging stage the model was cut and photographed. The individual layers of the model described with their physical characteristics are as follows (from bottom to top): a 5mm thick buoyant lower layer of Newtonian Rhodorsil Gomme (RG1, $\rho = 1.224 \text{ g/cm}^3$ and $\mu_{\text{eff}} = 8.5 \cdot 10^4 \text{ Pa s}$) simulating a partially molten magma ($\rho = 2.45 \text{ g/cm}^3$ and $\mu_{\text{eff}} = 8.5 \cdot 10^{18} \text{ Pa s}$), a 50mm thick non-Newtonian overburden mixture of Rhodorsil Gomme + Plastilina (RG+P, $\rho = 1.34 \text{ g/cm}^3$ and $\mu_{\text{eff}} = 10^6 \text{ Pa s}$) simulating a silicic overburden ($\rho = 2.7 \text{ g/cm}^3$ and $\mu_{\text{eff}} = 10^{20} \text{ Pa s}$) in nature and a 10mm thick layer of PDMS ($\rho = 0.964 \text{ g/cm}^3$ and $\mu_{\text{eff}} = 4 \cdot 10^4 \text{ Pa s}$) simulating a less dense overburden to prevent the diapirs from extruding. Scaling parameters are presented in Table 1. In order to govern the location of the diapir, a perturbation was initiated on top of the buoyant layer in the center of the model (Fig. 4).

The model was centrifuged for 9'30'' at 700 g before a profile was cut for photographing. Two mushroom-shaped diapirs of the buoyant layer intruded the overburden and spread below the less-dense PDMS layer (Fig. 5). One diapir developed at the perturbation site and another one developed at the margin of the model. Moreover, two smaller diapirs reached the surface of the model (Figs. 5a-b). A fifth diapir, which formed close to the opposite margin ceased rising after only 1 cm, probably as a result of shortage in supply of the buoyant material (Figs. 5c-d). During their rise, the diapirs deformed the overburden units. A strain grid on top of the model deformed significantly due to emplacement of the diapirs underneath the PDMS layer (Fig. 5a). Peripheral skirts developed at the rims of the two spreading diapirs, whereas intense folding developed in the overburden between these two diapirs. Moreover, although being less dense than the other two materials, the PDMS overburden was dragged downward between the two diapirs (Figs. 5c-d).

After photographing, the model was put together and welded by contact. A second buoyant layer of similar density and viscosity as the first buoyant layer, (differently stained RG2 layer) was attached to the bottom of the model. The model was then centrifuged for an additional 6'10'' at 700g.

During the centrifuging, a second-stage intrusion of the second buoyant material occurred. The intrusion of this buoyant material led to extensive spreading and expansion of the first stage diapirs, whose surface area increased by 25 to 50%. The two small diapirs unified to

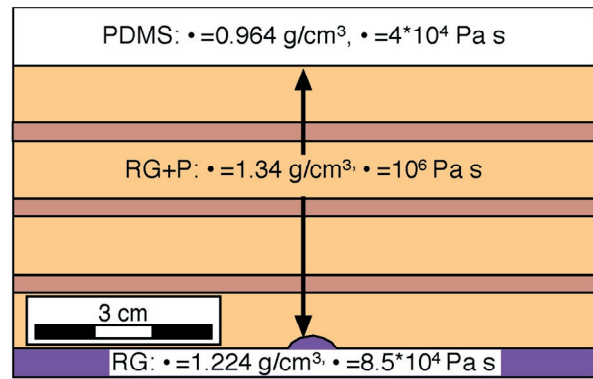


Figure 4. Initial set-up of the experiment (PDMS = polydimethyl-siloxane, RG = Rhodorsil Gomme bouncing putty, P = plastilina).

Quantity	model (m)	nature (n)	model ratios
Thickness of overburden (l_o)	50 mm	5000 m	$l_{mo}/l_{no} = 10^{-5}$
Thickness of buoyant layer (l_b)	5 mm	500 m	$l_{mb}/l_{nb} = 10^{-5}$
Density of overburden (ρ_o)	1.34 g/cm ³	2.45 g/cm ³	$\rho_{mo}/\rho_{no} = 0.50$
Density of buoyant layer (ρ_b)	1.224 g/cm ³	2.7 g/cm ³	$\rho_{mb}/\rho_{nb} = 0.50$
Viscosity of overburden (μ_o)	10 ⁶ Pa s	10 ²⁰ Pa s	$\mu_{mo}/\mu_{no} = 10^{-14}$
Viscosity of buoyant layer (μ_b)	8.5 * 10 ⁴ Pa s	8.5 * 10 ¹⁸ Pa s	$\mu_{mb}/\mu_{nb} = 10^{-14}$
Acceleration (g)	6867 m/sec ²	9.81 m/sec ²	$g_m/g_n = 700$

Table 1. Properties of the RG (Rhodorsil Gomme; buoyant) and RG+P (Rhodorsil Gomme + Plastilina; overburden) materials used in the presented model.

just one expanded diapir (Figs. 6a-b). As a result of this ballooning the diapirs were overthrust upon each other and upon the overburden (Figs. 6c-d). Internal flow within the diapirs led to peripheral skirts at the rims of the second stage intrusions. The RG2 material rose along the stem of the pre-existing diapirs, using them as mechanically weak pathways for its rise (Figs. 6c-d).

The results of the experiment can be summarized as follows. During the first stage of centrifuging, two mushroom-shaped diapirs of the buoyant RG1 layer intruded the overburden to spread below the less-dense PDMS layer. During their rise, the diapirs deformed the overburden units and caused the formation of rim synclines around the diapirs (Figs. 5b and d). During a second stage of centrifuging a second intrusion occurred within the stem of the pre-existing diapirs. Once reaching the level of neutral buoyancy, the intrusive material spread laterally resulting in expansion of the overhang of the pre-existing diapirs. This led to the formation of tabular intrusive bodies (Figs. 6b and d).

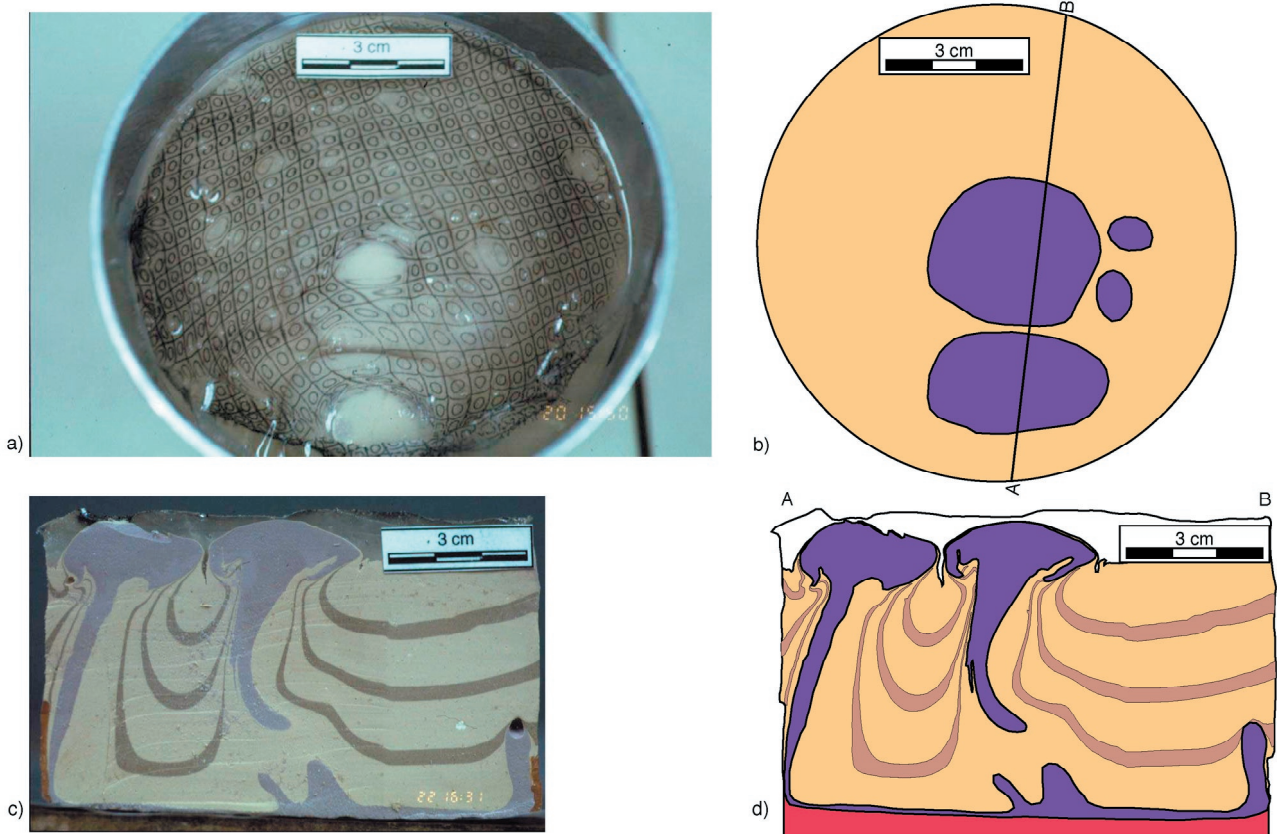


Figure 5. **a)** Map view photograph of the experiment after the first stage of the experiment (centrifuging time: 9'30"). Two large diapirs and two smaller ones have spread under the PDMS layer and a thin cover of RG+P. A strain grid on top of the model deformed significantly due to emplacement of the diapirs underneath the PDMS layer. **b)** Sketch of the situation shown in Fig. 5a. The heads of the diapirs appear in blue, the overburden in beige. The cross section shown in Figs. 5c and d follows the line A-B. **c)** Photograph of a cross section through the model along line A-B in Fig. 5b. after emplacement of the first -generation diapir (centrifuging time: 9'30"). The RG1 forms two mushroom-shaped diapirs beneath a thin coating of RG+P. A third diapir at the right edge of the model was aborted due to shortage in buoyant material. The passively stratified RG+P overburden was strongly deformed during the rise of RG1 and forms rim synclines around and inbetween the two diapirs. Even the less dense PDMS layer is affected by the emplacement of the two diapirs and was dragged downward as the diapirs spread at their level of neutral buoyancy. **d)** Drawing of the situation shown in Fig. 5c. In addition the red RG2 layer attached to the model is shown.

Discussion and conclusions

Both intrusion mechanisms proposed for CEPs, diapirism and dyking, have their strong and weak points. Dykes are efficient as transport conduits for the construction of sheeted plutonic complexes and it is even possible to construct dyke-fed magma chambers with a concentric internal fabric. However, it is not yet clear how magma ascent can be related to brittle – and at the tip of the crack - elastic process like fracturing (Weijermars 1997), while the emplacement is driven purely by ductile (i.e. plastic) processes (i.e. magma chamber expansion in combination with a ductilely deforming aureole). Diapirism, on the other hand, is a viable ascent and emplacement mechanism in the lower crust. It has been frequently debated, whether granitoids can rise as diapirs above the brittle-ductile boundary in the continental crust (e.g. Vigneresse and Clemens 2000).

The subsequent intrusions of nested diapirs into the same region or even magma chamber can extend the lifetime of an igneous system, because the consecutive intrusion of numerous melt bodies supplies additional heat and buoyant material, i.e. magma. Moreover, nesting

of diapirs suggests that the first intrusive bodies created pre-heated pathways for later batches of typically more felsic magma, allowing the latter to rise faster and with less heat loss. Consequently, nesting makes it possible for diapirs to ascend farther than modeled hot-Stokes diapirs (Miller and Paterson 1999), which according to Marsh (1982) cannot rise farther than twice their diameter. The present experiment shows how nesting of diapirs can work in a ductile regime. It also points to the fact that CEPs are not necessarily the result of diapirism *sensu strictu*.

The first intrusion in the experiment was clearly diapiric and evolved all the diapiric features known from former laboratory experiments (e.g. Ramberg 1981). Mushroom shape with the very thin stems is typical for diapirs developing when viscosity ratio between overburden and buoyant layer ($m = \mu_{\text{overburden}}/\mu_{\text{buoyant}}$) is ≈ 1 (Jackson and Talbot 1989). In the current experiment, this rate is 11.77. Dragging upward of the overburden material and the formation of rim synclines are also typical diapiric features (Figs. 5c-d).

The second buoyant layer (RG2) used the stems of the pre-existing diapirs as mechanically weak and conduit-like pathways. Use of these weak zones facilitated and

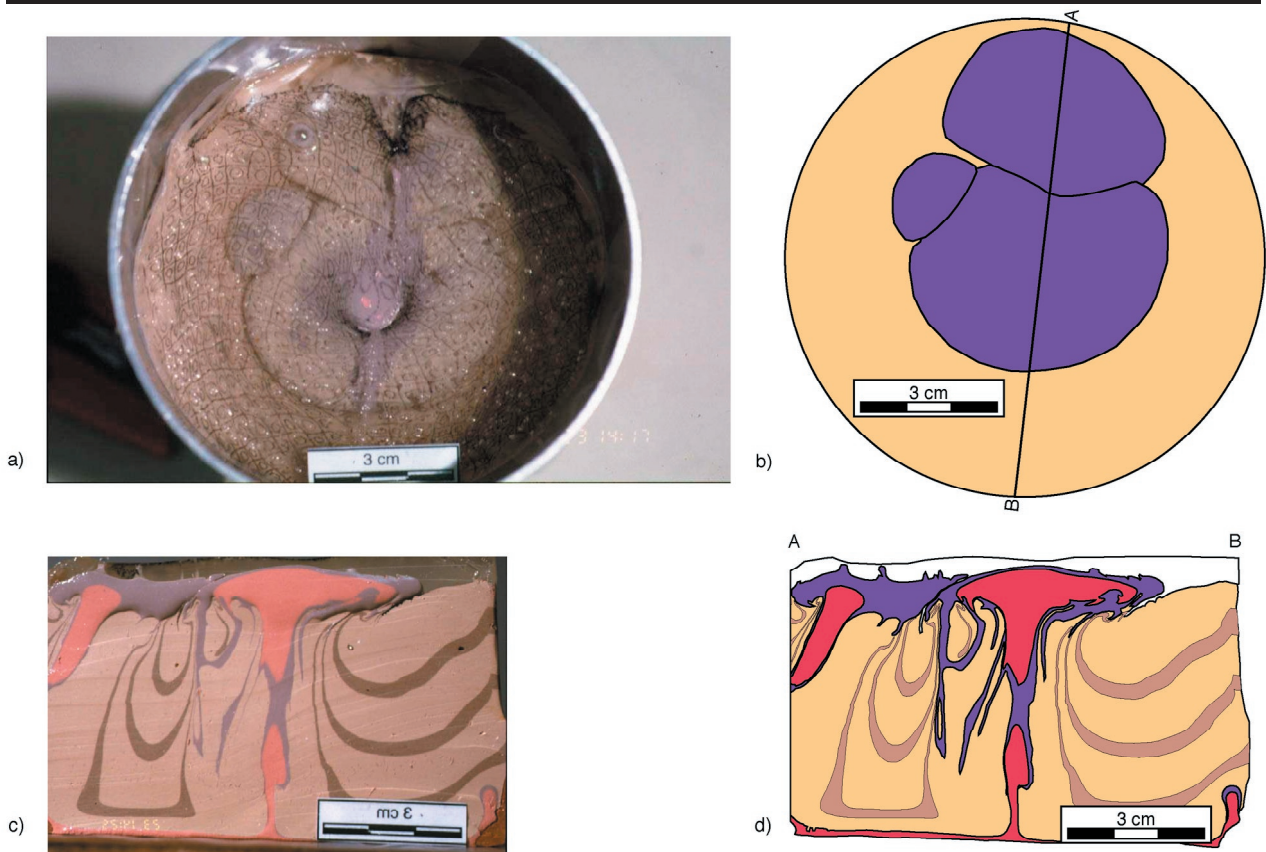


Figure 6. **a)** Map view photograph of the experiment after the second stage of the experiment (centrifuging time: 6'10"). The diapir bulbs have spread tremendously due to the emplacement of the buoyant RG2 material: the surface area of the diapir closest to point A along the profile line in Figs. 5b and 6b increased by 25% and the one in the centre of the model increased in size even by 50%. The two smaller intrusions obviously unified and form now one diapir whose surface area is 50% larger than the surface area covered by its two precursors. **b)** Sketch of the situation shown in Fig. 6 a). The heads of the diapirs appear in blue, the overburden in beige. The cross section shown in Figs. 6c and d follows the line A-B. **c)** Photograph of a cross section through the model along line A-B in Fig. 6 b) after emplacement of the RG2 intrusions (centrifuging time: 6'10"). The RG2 rose along the stem of the pre-existing diapirs using them as mechanically weak pathways. When reaching their level of neutral buoyancy, i.e. the bulb of the RG1 diapirs, the RG2 intrusions spread laterally leading also to an expansion of their precursors. The final shape of the entire intrusive complex is tabular. **d)** Drawing of the situation shown in Fig. 6 c).

accelerated the rise of RG2 compared to RG1. It took the first generation diapirs 9'30" to reach its level of neutral buoyancy and to spread beneath the PDMS layer, whereas the second intrusion needed at maximum 6'10".

Following the stems of the RG1 diapirs gives the ascending RG2 intrusions probably a dyke-like appearance with a large lateral extent relative to thickness, which is, according to Spera (1980), the main characteristics of dykes. Moreover, according to the definitions for diapirism and dyking used in this study, the use of a zone of weakness as a pathway is typical for dyking. Consequently, the second intrusion was not unambiguously diapiric, but shows some geometric features characteristic of dykes. However, dyking is a mechanism whereby a magma fractures the crust by using the elastic properties of rocks (Lister and Kerr 1991). In the experiment described above only viscous materials were applied, which do not behave elastically. To solve this dilemma and to describe the ascent mechanism of the RG2 layer we introduce the term "ductile dyking" as the buoyancy-driven rise of viscous body with a large aspect ratio through a viscous medium along weak pathways and by ductile processes. In fact, also in nature, as the host

rock will be deformed ductilely already during the first diapiric intrusion, "ductile dykes" rather than elastical fracturing of the host rock is more likely. Ductile dyking may leave some geochemical signature, which can be identified in the field and which might help distinguish it from dyking under brittle conditions. In case the earlier intrusions still contain melt, those can be mingling structures, back-veining of the older intrusive material and the incorporation of xenocrysts from the pre-intruded magma. In addition, since "ductile dyking" is associated with a relatively heated and hence ductile host rock, it is less likely to find chilled margins in "ductile dykes".

When reaching the bulbs of the pre-existing diapirs (i.e. the level of neutral buoyancy) the second stage intrusions spread and inflated the RG1 diapirs. The final shape of the nested diapirs is tabular as proposed by McCaffrey and Petford (1997) for most plutons. However, they are not the result of pure dyking and ballooning as suggested by these authors, but the outcome of combined diapirism, "ductile dyking" and ballooning. Transferred to nature, the results of the experiment imply that heavily deformed ductile aureoles form already during an early diapiric stage in the emplacement history of a CEP. Most internal fabrics

of CEPs are created when subsequent dyke-like magma pulses enter the magma chamber, inflate it and overprint the fabrics which developed during the first intrusive stage.

In nature, nesting of multiple magma bodies extends the life time of igneous systems, because their consecutive intrusion adds additional heat to the system which may enable CEPs to pass the ductile-brittle transition at about 10 km depth. That is shown by the Ardara pluton, Cannibal Creek pluton and Tuolumne intrusive suite, respectively, which all were emplaced above the ductile-brittle transition (Paterson and Vernon, 1995).

In conclusion, model results show that CEPs can form by a combination of diapirism and subsequent “ductile dyking” of buoyant material through the stem of pre-existing diapirs. Multiple diapirs can form only when the overburden units deform ductilely during the different stages of diapirism. Multiple injections of magma into the magma chamber lead to ballooning and to a kinematic reactivation of the igneous system. The consecutive intrusion of several magma batches (first by diapirism, followed by “ductile dyking”) extends the longevity of CEPs through the additional heat input of the individual subsequent intrusion and allows them to rise beyond the brittle-ductile boundary within the Earth’s crust.

References

- Bateman, PC (1992) Plutonism in the central part of the Sierra Nevada batholith, California. USGS Prof Paper, 1483.
- Bateman, PC, Chappel BW (1979) Crystallization, fractionation, and solidification of the Tuolumne Intrusive Series, Yosemite National Park, California: GSA Bull, 90: 456-482.
- Bateman, R (1985a) Aureole deformation by flattening around a diapir during in situ ballooning; the Cannibal Creek Granite. J Geol, 93: 293-310.
- Bateman, R (1985b) Progressive crystallization of a granitoid diapir and its relationship to stages of emplacement. J Geol, 93: 645-662.
- Bultitude, RJ, Champion, DC (1992) Granites of the eastern Hodgkinson province – their field and petrographic characteristics. Dep Resour Ind Rec 1992/6, Queensland Gov Publ.
- Jackson, MPA, Talbot, CJ (1989) Anatomy of mushroom shaped diapirs. J Struct Geol, 11: 211-230.
- Kerrick, DM (1987) Fibrolite in the contact aureoles of Donegal, Ireland. Am Min, 72: 240-254.
- Lister, JR, Kerr, RC (1991) Fluid-mechanical models of crack propagation and their application to magma transport in dykes. J Geophys Res, 96: 10049-10077.
- Marsh, BD (1982) On the mechanics of igneous diapirism, stopping, and zone melting. Am J Sci, 282: 808-855.
- McCaffrey, KJW, Petford, N (1997) Are granitic intrusions scale invariant? J Geol Soc London 154: 1-4.
- Miller, RB, Paterson, SR (1999) In defense of magmatic diapirs. J Struct Geol, 21: 1161-1173.
- Molyneux, SJ, Hutton, DHW (2000) Evidence for significant granite space creation by the ballooning mechanism; the example of the Ardara Pluton, Ireland. GSA Bulletin, 112: 1543-1558.
- Paterson, SR (1988) Cannibal Creek granite: Post-tectonic “ballooning” pluton or pre-tectonic piercement diapir? J Geol 96: 730-736.
- Paterson, SR, Vernon, (1995) Bursting the bubble of ballooning plutons; a return to nested diapirs emplaced by multiple processes. GS A Bulletin 107: 1356-1380.
- Petford, N (1996) Dykes and diapirs? Trans R Soc Edinburgh, Earth Sciences 87: 105-114.
- Pitcher, WS, Berger, AR (1972) The Geology of Donegal: A Study of Granite Emplacement and Unroofing. Wiley.
- Ramberg, H (1981) Gravity, Deformation and the Earth’s Crust. 2nd edition. Acad Press.
- Spera, FJ (1980) Aspects of magma transport. In: Hargraves, RB (ed) Physics of magmatic processes. Princeton Univ Press: 265-324.
- Tikoff, B, Teyssier, C (1992) Crustal-scale, en echelon “P-shear” tensional bridges; a possible solution to the batholithic room problem. Geology, 20: 927-930.
- Van den Eckhout, B, Grocott, J, Vissers, R (1986) On the role of diapirism in the segregation, ascent and final emplacement of granitoid magmas - Discussion. Tectonophysics 127: 161-169.
- Vignerresse, JL, Clemens, JD (2000) Granitic magma ascent and emplacement: neither diapirism nor neutral buoyancy? In: Vendeville, BC, Mart, Y, Vignerresse, JL (eds) Salt, Shale and Igneous Diapirs. Geol Soc London, Spec Publ, 174: 7-21.
- Weijermars, R (1997) Principles of rock mechanics. Alboran Sci Publ.